Published by
NIGERIAN SOCIETY OF PHYSICAL SCIENCES
available online @ https://jnsps.org

J. Nig. Soc. Phys. Sci. 2 (2020) 7–11

Journal of the Nigerian Society of Physical Sciences

Original Research

Preparation and Characterization of High Performance Dye Sensitized Solar Cells with Silver Nanoparticles in nanocomposite Photoanode

T. Jamila[a], E. Lucky[b], D. Eli[c,d,*]

[a]Department of Physics, Kaduna State University, Kaduna, Nigeria
[b]Department of Chemical Sciences, Greenfield University, Kaduna, Nigeria
[c]Department of Physics, Nigerian Defence Academy, Kaduna
[d]Department of Physical Sciences, Greenfield University, Kaduna, Nigeria

RETRACTED

Abstract

Surface plasmon resonance is the effect of electron oscillation in a structure stimulated by incident light. When noble materials such as *Ag*, *Au* or *Cu* are added into the titania (compact or mesoporous) structure of the sensitized solar cell, the plasmonic effect of such materials will result to an improved performance of the device. Placing *AgNP*s at different position will produce a variety of result. In this work the systematic design and formation of plasmonic dye sensitized solar cells (DSSCs) by integrating *AgNP*s nanoparticles (NPs) in two distinct configurations; on the $c - TiO_2$ and on $m - TiO_2$ were reported. The power conversion efficiency (PCE), Jsc and Voc of the reference device shows a value of 0.36 %, 1.89 $mAcm^{-2}$ and 0.45 V. Upon introduction of *AgNP*s on the $c - TiO_2$, a PCE of 0.64 %, Jsc of 2.53 $mAcm^{-2}$ and Voc of 0.46V were recorded, which improved the PCE ~63.90 % over that of the prestine device. When *AgNP*s is introduced on the $m - TiO_2$, a PCE of 0.71 %, Jsc of 2.83 $mAcm^{-2}$ and Voc of 0.46 V were obtained which results to increase in power conversion efficiency from 0.36 % to 0.71 %, demonstrating ≈ 1.97 time's enhancement, compared with the reference device without the metal NPs. The improvement is attributed to an increase in photocurrent density due to enhanced light harvesting by silver nanoparticles.

Keywords: DSSCs, Surface Plasmon, Nanoparticles, Natural Pigment

Article History :
Received: 30 November 2019
Received in revised form: 16 January 2020
Accepted for publication: 30 January 2020
Published: 28 February 2020

©2020 Journal of the Nigerian Society of Physical Sciences. All rights reserved.
Communicated by: W. A. Yahaya

1. Introduction

We can consider the issue of energy as a necessity being a fundamental problem facing the world and humanity today. Fortunately, as the earth receives abundant sunlight throughout the year, it is wise to harvest such alternative resource for energy conversion and consumption. One of the direct ways of harnessing solar energy is through solar cell. Sequentially, solar cell technologies have developed into three generations [1, 2]. The first generation photovoltaic solar cell is based on a single crystalline semiconductor wafer. The second era solar cells use thin layer of polycrystalline semiconductor, they are less expensive to produce, adaptable and lightweight; however, the performance is still lower than the first generation cells. The third era solar cell is a new minimal chemical solar cell that was accomplished by the combination of nanostructured electrodes and proficient charge injection dyes [3, 4]. The recent devel-

*Corresponding author tel. no: +2348063307256
Email address: danladielibako@gmail.com (D. Eli)

opment of solar cell technologies has provided much hope in the renewable energy field due to their ease of fabrication and low cost [5, 6, 7, 8]. To date, the highest reported efficiency of DSSC is about 14 % [9]. Recently, solar cell structure with high performing perovskite as sensitizer has emerged as a new breakthrough in the solar cells field where efficiency as high as > 23 % has been reported [10, 11, 12].

The main working mechanism of DSSC relies on the photon absorption by the sensitizers followed by the transfer of photogenerated electrons within the circuit. However, increasing power conversion efficiency further to realize the outdoor applications are still one of the crucial issues in DSSC research. The absorption process can be enhanced with the inclusion of noble metal nanoparticles in the TiO_2 compact and mesoporous structure, acting as scattering centers and sub-wavelength antennas [13]. It is worth mentioning that for noble metal nanoparticles to have significant positive effect in solar cells, the non-radiative transfer between the photoactive layer and nanoparticles must be reduced [3, 14]. Noble materials such as Ag, Cu or Au nanoparticles are thought to enhance the photocurrents of DSSC as a result of localized surface plasmon resonance (LSPR) effect of the nanoparticles [15]. In general, surface plasmon resonance is the effect of electron oscillation in a structure stimulated by incident light. The effect of the LSPR on Ag, Cu or Au nanoparticles results in enhanced light absorption and scattering which ultimately enhances the performance of DSSC.

In this work, we demonstrated the use of silver nanoparticles with average size of 16 *nm* deposited on the $c - TiO_2$ and $m - TiO_2$ to produce a film for the photoanode of DSSCs. Ag was selected due to its advantages as high conductor, and chemical and thermal stability [3, 8]. Natural pigment from delonix regia was then used as the sensitizer in a sandwich type DSSC.

2. Materials and Methods

2.1. Synthesis of Ag nanoparticles

To fabricate the silver NPs, a modified two-step reduction synthesis procedure was implemented, which was developed based on the conventional reduction method [16, 17]. We first heat the mixture containing sodium borohydride ($NaBH_4$) and tri-sodium citrate (TSC) at the ratio of 2:7 (1×10^{-3} $moldm^{-3}$: 3.5×10^{-3} $moldm^{-3}$) to 60 $^{\circ}C$ at 300 rpm for 30 min under vigorous stirring to ensure a formation of homogenous solution. 45 min later, 4 ml of an aqueous solution of $AgNO_3$ (4×10^{-3} $moldm^{-3}$) was added drop-wise to the mixture, and the temperature was further raised to 100 $^{\circ}C$ to make the solution boil quickly. The reaction was allowed to continue for another 45 min. Finally, the solution was cooled down to room temperature with stirring, and the NPs were collected by centrifugation at 5000 rpm and redispersed in ethanol via sonication for 15 min.

2.2. Extraction of dye pigment

The flame tree flower (*delonix regia*) was collected in plastic rubber from flamboyant tree. The flame flower was separated from its stalk. The sample was crushed via the use of a porcelain mortar and pestle. The sample, was filtered and stored in test tubes. The filtrate (extract) is the dye solution for sensitization.

2.3. Solar Cells Preparation

Fluorine doped tin oxide (FTO) (sheet resistance 8 $\Omega square^{-1}$, Solaronix) was used as a substrate for both photoanode and counter electrode. 0.38 M di-isopropoxytitanum bis(acetylacetonate) in ethanol was spin-coated at 3000 rpm for 10 s on the photoanode FTO. This was followed by sintering at 450 $^{\circ}C$ for 30 min to form a compact layer. The TiO_2 mesoporous layer was deposited by screen printing. It was then sintered in air for 30 $mins$ at 500 $^{\circ}C$.

For samples with the inclusion of Ag nanoparticles, the Ag nanoparticles was deposited on the $c - TiO_2$ and $m - TiO_2$ through SILAR procedure. It was then sonicated for about 20 $minutes$ to ensure homoegenous distribution of the Ag nanoparticles on $c - TiO_2$ and $m - TiO_2$ particles. All the as prepared photoanodes were soaked overnight in 0.2 mM delonix regia dye.

Counter electrode was prepared by spin coating a Pt catalyst (Solaronix) on FTO. The Pt coated FTO was then sintered at 500 $^{\circ}C$ for 30 min.

The iodide-based liquid electrolyte used was prepared following the method earlier described by Jun *et al.* [1]. It involves 0.6 M 3-propyl-1-methylimidazolium iodide, 0.1 M lithium iodide, 0.05 M iodine and 0.5 M 4-tert-butylpyridine in acetonitrile. A parafilm spacer was used to contain the liquid electrolyte within the cell assembly.

Solar cell assembly was done by sandwiching the liquid electrolyte between the sensitized electrode and Pt counter electrode.

2.4. Characterization and Measurement

The current density-voltage (J-V) characteristics of the cells were recorded using a setup comprising a xenon lamp, an AM 1.5 light filter, and an Electrochemical Analyzer (Keithley 2400 source meter) under an irradiance of 100 mW/cm^2 illumination from a Newport A solar simulator. Scanning Electron Microscopy (SEM) images were obtained using Carl Zeiss at an acceleration voltage of 20 kV. Visible region extinction spectra of dye, electrodes without dye and electrodes with dye were recorded on Axiom Medicals UV752 UV-vis-NIR spectrophotometer. The cell active area was 0.50 cm^2.

3. Materials and Methods

3.1. SEM Morphologies of TiO_2, $c - TiO_2 : AgNPs$ and $c - TiO_2 : AgNPs$

The SEM surface morphologies of the TiO_2, $c - TiO_2 : AgNPs$ and $m - TiO_2 : AgNPs$ composite films are shown in Fig. 1(a)-(c). The SEM images show little difference between films with $AgNPs$, and all films showed compact morphologies and smooth surfaces.

By using semiquantitative energy dispersive X-ray spectroscopy, peaks associated with Ti, O, Ag, Ar, N, Cd, C, Ca, Cl,

RETRACTED

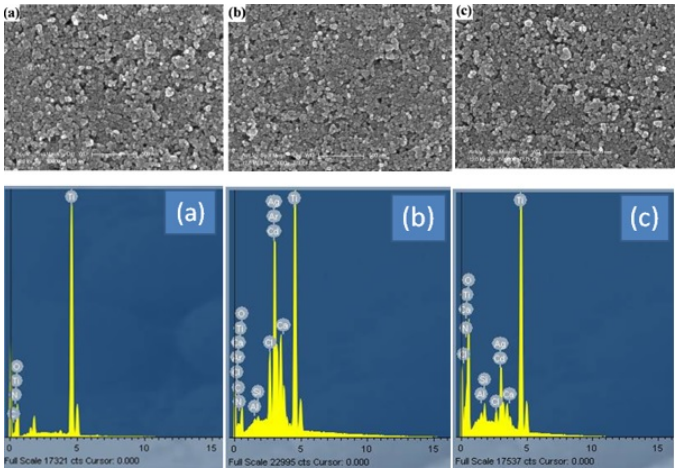

Figure 1: SEM and EDX micrographs of (a) TiO_2, (b) $c-TiO_2 : AgNPs$ and (c) $m - TiO_2 : AgNPs$.

Al and Si are clearly observed in the five spectra. The Ti and O peaks confirmed the presence of TiO_2 particles, and Ag peak obviously resulted from Ag nanoparticles. A very low peak ascribed to Al element is probably related to the specimens' manipulations during SEM investigation. The signal of Si, Ca, Ar and Cd should be attributed to the building element of the substrate since no other Si, Ca, Ar or Cd-based chemicals were used throughout the synthesis. The presence of C in Figure 1(a) most probably originates from Na-PAA traces involved during the synthesis.

3.2. Microstructures of the Photoanodes

Fig. 2 shows the XRD patterns of the TiO_2, $c - TiO_2 : AgNPs$, and $m - TiO_2 : AgNPs$ films. The patterns showed that all films had good crystallinity. The characteristic peaks of (101), (200), (105) and (211) for anatase and (110) for rutile were observed in these patterns, indicating the coexistence of the anatase and rutile phases in the TiO_2. Besides these, characteristic peaks of Ag (111) and (104) were also observed in the patterns of the TiO_2 modified with $AgNPs$ composite films, suggesting the stable existence of $AgNPs$ in composite films. It can also be seen that, the intensity of the anatase (101) peaks of the TiO_2 film increased with introduction of $AgNPs$, showing higher crystallinity of the films compared to that of the unmodified TiO_2. A peak at (004) corresponding to the rutile phase was also observed in the patterns of TiO_2 with $AgNPs$ films, suggesting a possible increase of the rutile phase in TiO_2. The properties demonstrated with the modified photoanode would enhance light scattering and absorption [18], which may enhance the photovoltaic properties of the DSSCs.

3.3. UV-visible spectroscopy

Figure 3(a) shows the absorption of the natural pigment that serves as light harvester in this research within the wavelength range of $200 - 1200\ nm$. From the Figure, the harvester displays absorbing properties between 400 to 600 nm with two distinct peaks of absorption noticed at $\approx$ 450 and $\approx$ 550 nm.

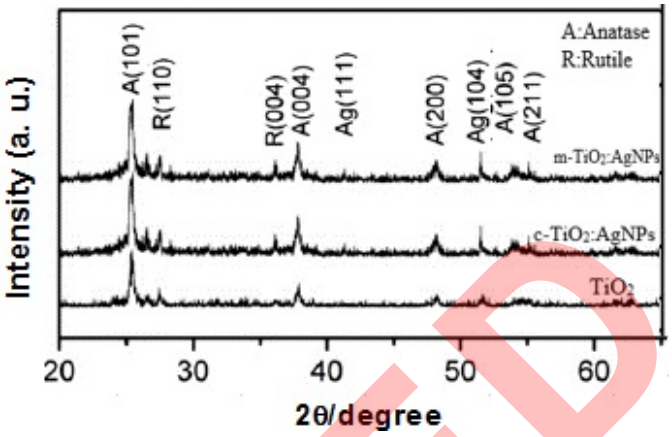

Figure 2: XRD pattern of (a) TiO_2, (b) $c - TiO_2 : AgNPs$ and (c) $m - TiO_2 : AgNPs$.

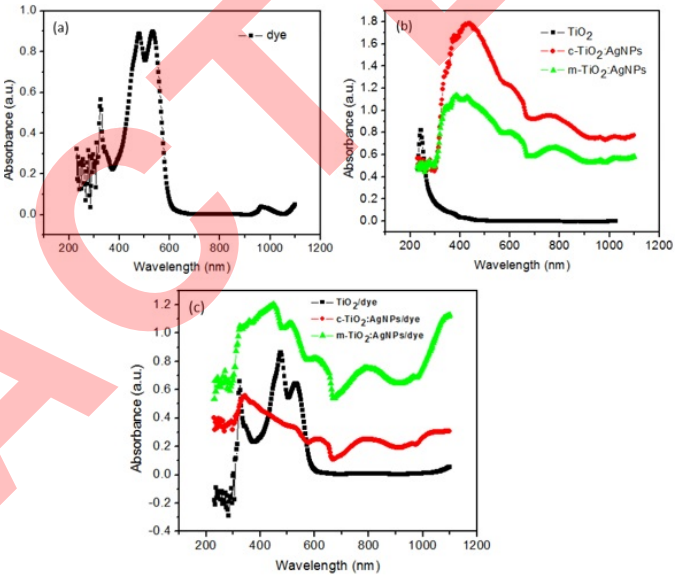

Figure 3: The absorption-wavelength of (a) natural pigment, (b) TiO_2, $c-TiO_2$ and $m-TiO_2$ without dye and (c) TiO_2, $c-TiO_2$ and $m-TiO_2$ with dye.

The absorption at the visible region demonstrates the satisfaction of the sample as light harvester in this research. Figure 3(b) shows the absorbance-wavelength plot for TiO_2, $c - TiO_2$ and $m - TiO_2$ without dye pigment. As seen, no absorption peak seen within the Vis-NIR region with TiO_2. We also observe a sharp peak around 316 nm within the UV region of TiO_2 due to electronic transitions between molecules having an intermediate ionic degree. The absorptivity at the UV region affirmed to the necessity of modifying the TiO_2 to make it active under visible light. After modification of TiO_2 (compact and mesoporous) with $AgNPs$, absorption enhancement was noticed on the $AgNPs$ - TiO_2 modified samples. This shows that modification of TiO_2 with $AgNPs$ causes a deformation in the network of the film thereby resulting to redshift in the optical band edge. Also resonances were exhibited between 360 nm to 850 nm after sensitizing with natural pigment which demonstrate a red

RETRACTED

shift at the resonance (Figure 3(c)). As shown, the slightly red shifted extinction spectrum of the dye soaked samples as compared to the unsoaked samples is expected from the change in the LSPR which slightly shifts to longer wavelength upon the bond formation between the nanoparticles and the dye. In addition, the absorption intensity increase as the dye was sensitized on the samples. This behavior was usually ascribed to Ag^0 nanoparticles inducing visible light absorption [3, 15, 16]. Moreover, absorption bands at $400 - 500\ nm$ may also be attributed to Ag clusters.

3.4. Photovoltaic performance

DSSCs were fabricated and their J-V curves behavior were investigated. Their performance parameters were obtained from the J-V and P-V curves following equations 1 and 2 respectively [3].

$$FF = \frac{J_{max} \times V_{max}}{J_{sc} \times V_{oc}} \tag{1}$$

$$\eta = \frac{FF \times J_{sc} \times V_{oc}}{P_{IRRADIANCE}} \cdot 100\% \tag{2}$$

FF is Fill Factor, η is solar cell efficiency, $Vmax$ is maximum voltage, $Jmax$ is maximum current density, Jsc is short circuit current density, Voc is open circuit voltage and $P_{IRRADIANCE}$ is light intensity.

Figure 4(a) shows the J-V curves of all the DSSCs samples while Figure 4(b) shows the P-V curves of the formed DSSCs. The individual results are also tabulated in Table 1. The normal DSSC, i.e. cell without the inclusion of Ag nanoparticles, achieves an efficiency of 0.36 %. Its photocurrent density, Jsc and open circuit voltage, Voc are 1.89 $mAcm^{-2}$ and 0.45 V respectively. The measured J-V curve of the control sample has a fill factor value of 42 %.

With the introduction of Ag nanoparticles on TiO_2. The cell performance improved substantially. Device with $AgNP$s on $c-TiO_2$ shows an improved efficiency of 0.64 % while the best performance was obtained in the cell with $AgNP$s on $m-TiO_2$. The measured efficiency for the cell is 0.71 %, $\approx$ 2.0 times improvement compared with that without Ag nanoparticles. The improved efficiency was largely attributed to the increased Jsc due to the intensified near field effect resulting from the silver nanoparticles. Addition of $AgNP$s on the $m - TiO_2$ create a schottky barrier thus seen to reduce the e–h recombination centers generally attributed to the oxygen vacancies in TiO_2 in the surface layers [19]. Also, the Ag plasmon mode energetically overlaps with dye absorption zone possibly rendering charge into the TiO_2 nanoparticles.

However, when $AgNP$s is added to $c - TiO_2$, we also observed an enhancement compared to the reference device but not as pronounced as observed in the device with $AgNP$s on $m - TiO_2$, therefore, cell with $AgNP$s on $m - TiO_2$ is the optimum composition in order to get the maximum plasmonic effect of the Ag nanoparticles in our work.

Due to the decay of a strong local magnetic field from the Ag surface when it is coated on the $c - TiO_2$ layer, only fewer dye molecules were enhanced to promote charge separation and dissociation [14, 16]. It caused an apparent decrease of the optical absorption of dye, resulting in a limited enhanced photocurrent.

Also a smaller Schottky barrier in the interfacial region of Ag and TiO_2, attributed to a little difference between the work function of silver, 4.12 eV, and the electron affinity of TiO_2, 4.0 eV, had barely small influence on photocurrent in the visible region to match closely with the record for the standard electrode [16, 20]. Also the electrons from metal particle cannot efficiently be transported in the network and the scattering study showed that in this case specular reflectivity is maximized, thus preventing a fraction of light to penetrate the device while the light scattering to non-specular directions is not sufficient enough [16].

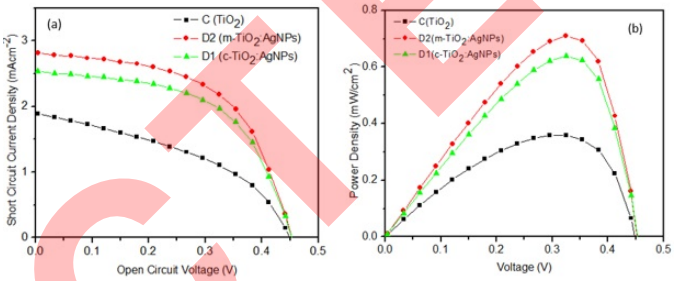

Figure 4: (a) J-V curves and (b) P-V curves of the control, C, D1, D2 devices.

Figure 4(b) shows the P-V curves of the control, C, D1, D2 devices. Their maximum powers are observed at 0.36, 0.64 and 0.71 $mWcm^{-2}$.

Figure 5 shows the plot of solar cell parameters; Voc, Jsc, FF and PCE with respect to the device. Observation shows that PCE, Jsc maximum values are at 0.71 % and 2.83 $mAcm^{-2}$ which was displayed by device D2. Device D1 demonstrates the highest FF with value 0.55.

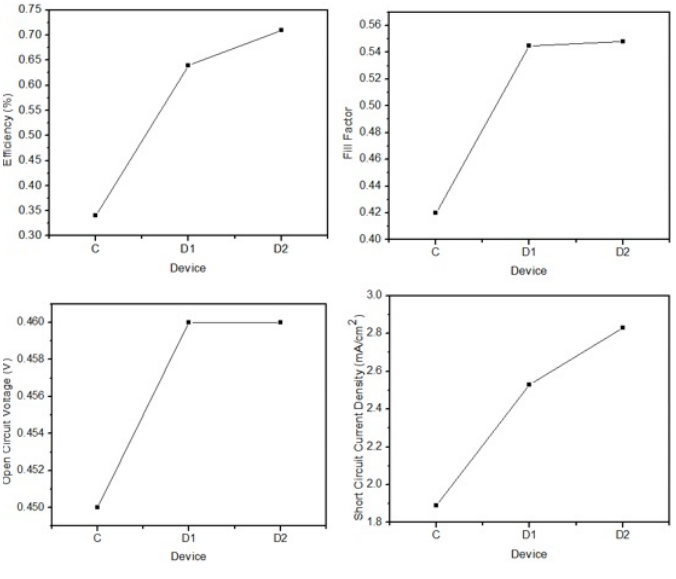

Figure 5: The curve of solar cell parameters; Voc, Jsc, FF and PCE with respect to the device.

RETRACTED

Table 1: Photovoltaic performance of $AgNP$s modified and unmodified PSCs under 100 $mWcm^{-2}$.

Device	Jsc($mAcm^{-2}$	Voc(V)	FF(%)	η	Enhancement
Control Device	1.89	0.45	42	0.36	0
D1	2.53	0.46	55	0.64	$\approx$ 1.80 times
D2	2.83	0.46	54	0.71	$\approx$ 2.00 times

4. Conclusion

The influence of $AgNP$s on the structure and performance of $Ag - TiO_2$ composite photoanodes and DSSCs was investigated. The results demonstrated that adding $AgNP$s to TiO_2 photoanodes significantly improved the performance of the DSSCs by increasing short-circuit current and open-circuit voltage. The best performing DSSC has $AgNP$s on the $m - TiO_2$ and gave a Jsc of 2.83 $mAcm^{-2}$, a Voc of 0.46 V and a photoelectric conversion efficiency of 0.71 %, greatly superior to that of DSSC using pure TiO_2 photoanode. The increase of Jsc is attributed to the enhanced light absorption and broadened absorption spectral range of the composite photoanode due to the SPR of the $AgNP$s.

Acknowledgments

We thank the referees for the positive enlightening comments and suggestions, which have greatly helped us in making improvements to this paper.

References

[1] H. K. Jun, M. A. Careem & A. K. Arof "Quantum dot-sensitized solar cells perspective and recent developments: A review of Cd chalcogenide quantum dots as sensitizer", Renewable and Sustainable Energy Reviews, **22** (2013) 148.

[2] J. H. Werner "Second and third generation photovoltaics–dreams and reality", Advances in Solid State Physics, **44** (2004) 51.

[3] D. Eli, G. J. Ibeh, O. O. Ige, J. A. Owolabi, R. U. Ugbe, B. O. Sherifdeen, M. Y. Onimisi & H. Ali "Silver Nanoparticles as Nano Antenna for TiO_2 Activation and its Application in DSSC for Enhanced Performance", Journal of Theoretical and Applied Physics, **1** (2019) 88.

[4] M. Y. Onimisi, D. Eli, S. G. Abdu, H. O. Aboh & J. Ezeoke "Size Effects of Silver Nanoparticles on the Photovoltaic Performance of Dye Sensitized Solar Cells", American Chemical Science Journal, **13** (2016) 1.

[5] D. Eli, P. M. Gyuk, M. S. Ahmad, G. I. Baba & S. H. Sarki "Silver Nanoparticles as Artificial Antennas for Enhanced Light-Harvesting and Charge Transfer in Dye-Sensitized Solar Cells", International Journal of Materials Science and Applications **5** (2016) 214.

[6] C. Chambers, S. B. Stewart, B. Su, H. F. Jenkinson, J. R. Sandy & A. J. Ireland, "Silver Doped Titanium Dioxide Nanoparticles as Antimicrobial Additives to Dental Polymers" Dental Materials, **33** (2017) 115.

[7] G. Kovacs, Z. Pap, C. Cotet, V. Cosoveanu, L. Baia & V. Danciu, "Photocatalytic, Morphological and Structural Properties of the TiO_2-SiO_2-Ag Porous Structures based System", Materials **8** (2015) 1059.

[8] D. Eli, A. A. Kassimu & B. O. Sherifdeen, "Surface-Enhanced Response of Silver Nanoparticles with SiO_2 and TiO_2 Core Shell for Enhanced dye Sensitized Solar Cells Performance: A Comparative Studies", Journal of the Nigerian Association of Mathematical Physics **43** (2017) 311.

[9] M. A. Green, K. Emery, Y. Hishikawa, W. Warta, E. D. Dunlop, D. H. Levi & A. W. Y. Ho-Baillie "Solar Cell Efficiency Tables (version 49)", Progress in Photovoltaics, **25** (2017) 3.

[10] L. Shuhan, Z. Xiangyu,W. Bao, Q. Yu, L.Wenhui, Y. Hao, L. Nan, C. Mengwei, L. Haifei & Y. Yingping, "Influence of Ag Nanoparticles with Different Sizes and Concentrations Embedded in a TiO_2 Compact Layer on the Conversion Efficiency of Perovskite Solar Cells", Nanoscale Research Letters, **13210** (2018) 1.

[11] W. S. Yang, B. W. Park, E. H. Jung, N. J. Jeon, Y. C. Kim, D. Lee, S. S. Shin, J. Seo, E. K. Kim, J. H. Noh & S. I. Seok, "Iodide Management in Formamidinium-Lead-Halide-Based Perovskite Layers for Efficient Solar Cells", Science, **356** (2017) 1376.

[12] Z. Lu, X. Pan, Y. Ma, Y. Li, L. Zheng, D. Zhang, Q. Xu, Z. Chen, S. Wang & B. Qu, "Plasmonic-Enhanced Perovskite Solar Cells using Alloy Popcorn Nanoparticles", RSC Advances, **5** (2015) 11175.

[13] D. Eli, M. Y. Onimisi, S. G. Abdu P. M. Gyuk & E. Jonathan, "Enhanced Performance of a Dye Sensitized Solar Cell using Silver Nanoparticles Modified Photoanode", Journal of Scientific Research & Reports, **10** (2016) 1.

[14] D. Eli, M. S. Ahmad, A. B. Bikimi & O. A. Babatunde, "Plasmonic Dye Sensitized Solar Cells Incorporated with $TiO_2 - Ag$ Nanostructures", International Research Journal of Pure and Applied Chemistry, **11** (2016) 1.

[15] D. Eli, J. A. Owolabi, O. O. Gabriel & E. Jonathan, "Plasmon-Enhanced Efficiency in Dye Sensitized Solar Cells Decorated with Size - Controlled Silver Nanoparticles Based on Anthocyanins as Light Harvesting Pigment", Journal of Photonic Materials and Technology, **2** (2016) 6.

[16] D. Eli & P. M. Gyuk "High Efficiency dye Sensitized Solar Cells by Excitation of Localized Surface Plasmon Resonance of $AgNPs$", Science World Journal, **14** (2019) 125.

[17] S. Agnihotri, S. Mukherji & S. Mukherji "Size-controlled silver nanoparticles synthesizedover the range 5–100 nm using the same protocoland their antibacterial efficacy", RSC Advances, **4** (2014) 3974.

[18] K. L. Kelly, E. Coronado, L. L. Zhao & G. C. Schatz, "The Optical Properties of Metal Nanoparticles: The Influence of Size, Shape, and Dielectric Environment", J. Phys. Chem. B, **107** (2003) 668.

[19] S. Muduli, O. Game, V. Dhas, Vijayamohanan, K. Bogle, K. A., Valanoor & S. B. Ogale "TiO_2–Au plasmonic nanocomposite for enhanced dye-sensitized solar cell (DSSC) performance", Solar Energy, **86** (2012) 1428.

[20] G. Zhao, H. Kozuka & T. Yoko "Sol—gel preparation and photoelectrochemical properties of TiO_2 films containing Au and Ag metal particles", Thin Solid Films, **277** (1996) 147.

RETRACTED